Supporting Informations for "Covalency and magnetic anisotropy in Lanthanide Single Molecule Magnets: the DyDOTA Archetype"

Matteo Briganti,[a] Guglielmo Fernandez Garcia,[a,b] Julie Jung,[b] Roberta Sessoli,[a] Boris Le Guennic,*[b] and Federico Totti*[a]

[a]Dipartimento di Chimica "U.Schiff" and UdR INSTM Università degli Studi di Firenze, Via della Lastruccia 3-13, 50019 Sesto Fiorentino (Italy)

[b]Université de Rennes, CNRS, ISCR (Institut des Sciences Chimiques de Rennes) - UMR 6226, F-35000 Rennes (France)

E-mail: boris.leguennic@univ-rennes1.fr, federico.totti@unifi.it

Contents

Description of the Models

In this section the different models used in the paper are defined in details to make the reader fully aware of the different account of the environment by geometrical and electrostatic point of view.

Model M1. In order to reduce at the minimum the number of bias inherent the choice of the model, we have considered a $[Dy(DOTA)(H_2O)]^-$ complex surrounded by four crystallographically symmetry related replicas along with the five Na^+ cations and the twenty-five co-crystallized water molecules (see Fig. S2) representing two unit cells and half. Such a choice was driven by the fact that the $[Dy(DOTA)(H_2O)]^-$ complexes form chains quite distant one from the other and only water molecules and Na^+ ions are present in between them. The whole model is formed by 414 atoms. However, such a model cannot be handled at the high level of theory as CASSCF/CASSI-SO approaches and, therefore, we chose to treat only one $[Dy(DOTA)(H_2O)]^+$ unit (56 atoms) explicitly and at the highest level while all the other atoms were considered as point charges (see Computational section for more details). The net total charge is almost neutral (Q1 = 0.11).

In this framework, the closest groups the two H_{AWM} can interact with are represented by two carboxyl groups belonging to adjacent DOTA molecules present in the cell. The distance between the closest oxygen atoms of the two carbonyl groups and the O_{AWM} are 2.773 and 2.803 $\AA$. Similar distances are also observed for the four oxygens of the DOTA ligand directly coordinating the Dysprosium ion (see Fig. S1). The two H_{AWM} are located in a network of an almost equidistant oxygens atoms theoretically eligible for hydrogen bonding. However, only the two oxygen atoms belonging to the adjacent DOTA ligands can be able to orient the O_{AWM}-H_{AWM} bonds at very low temperature.

For this reason, we have relaxed the H_{AWM} positions at the DFT level (see Compu-

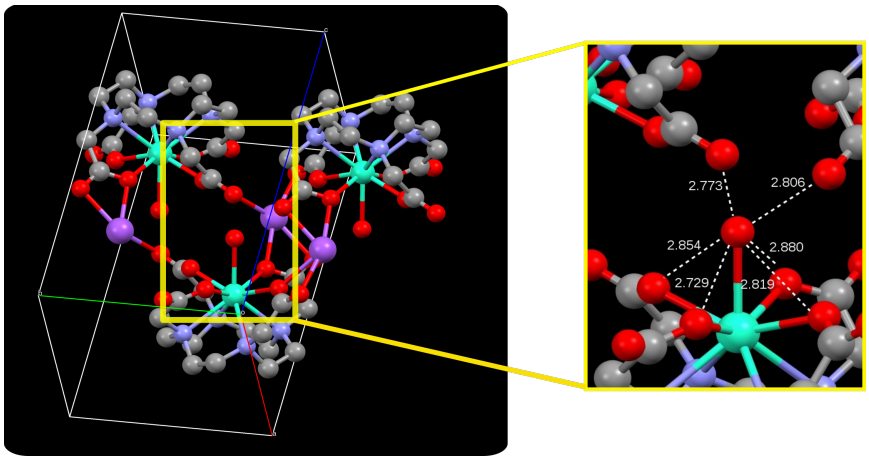

Fig. S1: Positions of the nearest carboxyl groups in the crystal cell of DyDOTA in $\AA$.

tational details). The dihedral angle φ, defined by the plane determined by the water molecule and pseudo C_4 passing through the Dysprosium ion was optimized to 36°. Such a value strongly deviates from what previously reported by Cucinotta *et al.*[1] (0°) where the two carboxyl groups where not considered in the optimization model, and by Blackburn[2] (22°), where the solution structure of $[Lu(DTMA)(H_2O)]^{3+}$ derivative was optimized in the gas phase. The two optimized O_{AWM}-H_{AWM} distances are 0.967 and 0.969 $\AA$, respectively. Such a geometry corresponds to $\alpha = 0°$, where α is the angle corresponding to the rigid rotation of the two optimized H_{AWM} atoms along the Dy-O_{AWM}. The angle α can, therefore, assume values from 0° (optimized H_{AWM} positions) to 2π values. We have also introduced the angle γ_n as a deviation index between the computed and experimental easy axis of magnetization, where n can assume values 0 and 1 for the ground and first excited Kramers' doublets, respectively.

Model M2 and M2m. With the aim to reduce the computational efforts but to have the same accuracy of **M1**, we reduced it to a model consisting of only one $[Dy(DOTA)(H_2O)]^-$ unit. Such a model represents the most intuitive, and therefore, the simplest possible model. The net total charge of the model, Q2, is -1. In order to mimic the intermolecular interactions in the crystal, the two carboxylates groups belonging to the two $[Dy(DOTA)(H_2O)]^-$

neighbour units that interact with the two H_{AWM}'s were modeled with two molecules of formaldehydes, as shown in Fig. S3 (Model 2, **M2**). The net total charge of the model is therefore maintained (Q2 = -1). The coordinates of two H_AWM atoms where left to relax and, in support of the goodness of the model proposed, no changes were computed for the O_{AWM}-H_{AWM} distances and φ angle.

In virtue of the simplicity of the model such a model has been used to performed the majority of the magnetic-structure calculations. Indeed, calculations for φ values of 0° and 90° where also computed for α = [0°, 90°]. It is worth to be mentioned that, the case for φ = 0° corresponds to the Model C used in the paper by Cucinotta *et al.*[1] and it has been then used as cross reference, too.

A simpler model (Model C in Cucinotta *et al.*[1]) where only the $[Dy(DOTA)H_2O]^-$ complex is also considered (i.e. no aldehydes added) is Model 2 'modified' (**M2m**). Such a model allowed to verify the role of the aldehydes.

In order to show the extreme difficulty to choose a structural model in which the experimental balance between electrostatic and orbital contributions can be reliably modeled we have built up three more models resembling the ones already used in literature.

Model M3. In the unit cell, each DyDOTA complex is surrounded by three counter-ions. Indeed, three of the four carboxylates involved in the coordination of the Dysprosium ion contribute to the coordination of three Na^+ ions, too. The Model 3 (**M3**, see Fig. S4) has been designed to account these three cations, positioned in their crystallographic positions. Moreover, to reduce the charge of system, the two aldehydes groups were substituted with two formate anions. The formates are in the same positions of the two carboxilate groups of the two next DOTA molecules in the crystal packing. This model is neutral (Q3 = 0) and it is composed by 67 atoms. The two H_{AWM} atoms were positioned accordingly to **M1**. All the atoms are considered explicitly. Such a model corresponds to Chilton's[3] model with the only difference related to the inclusion of the formates. For computational details see

computational methods.

Model M4. Model 4 is obtained adding to **M3** four more formate anions and the two water molecules around the three Na^+ ions (see Fig. S5). The added four formate groups mimic the carboxylate groups that belong to the DOTA ligands of the four neighbour DyDOTA complexes. The first coordination sphere of each Na^+ ion is now complete being coordinated by six oxygen atoms, differently from **M3**. However, the net total charge of the complex is -4 (Q4 = -4). The number of atoms in the model increased up to 92. The two H_{AWM} atoms were positioned accordingly to **M1**. All the atoms are considered explicitly. For computational details see computational methods.

Model M5. Each DyDOTA complex has got other four symmetry related DyDOTA complexes as first neighbours. To reduce the charge unbalance in **M4**, the computed DFT point charges of the four Dysprosium ions belonging to the surrounding complexes were added (see Fig. S6) to it (**M5**). The charge of the peripheral lanthanide ions was set to 1.37 and the net total charge, Q5, became 1.48. The two H_{AWM} atoms were positioned accordingly to **M1**. All the atoms are considered explicitly but the four neighbour Dy(III) ions. For computational details see computational methods. Such a model is very close to the Model A/A' (neutral charge) proposed by Cucinotta *et al.*[1] where acetates where used instead of out formiates and four excplicit Na^+ ions were used at the place of Dy(III) ions.

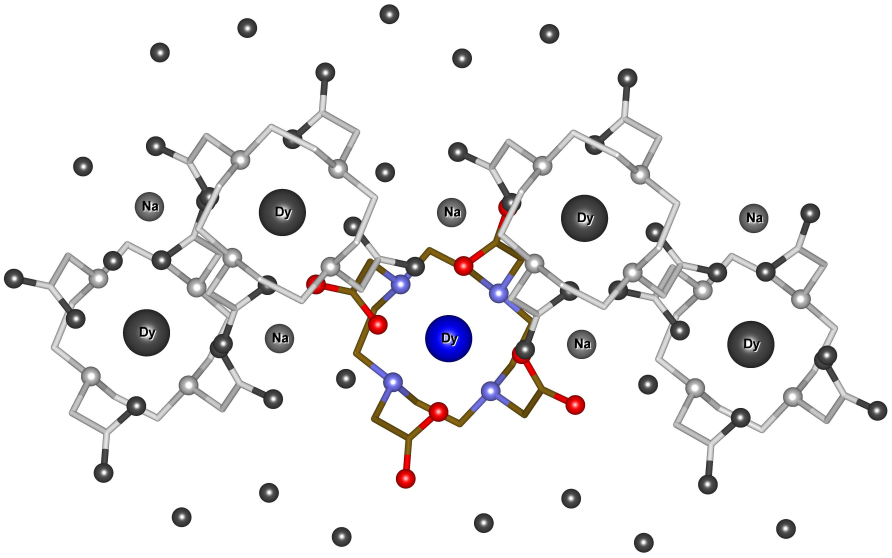

Fig. S2: Model **M1**. Dy, N, O, C are blue, pale blue, red and brown, respectively. The atoms in grey are substitued by their atomic point charges. Hydrogens atoms are hidden for sake of clarity.

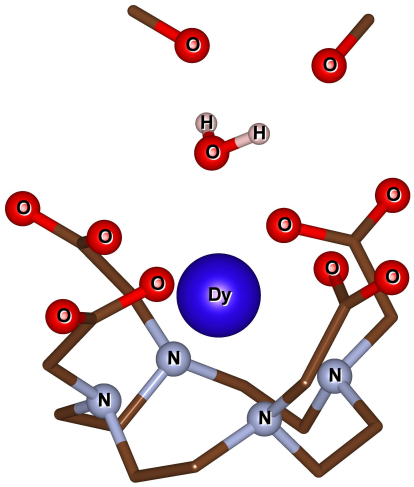

Fig. S3: Model **M2-2m**. Only the hydrogens of the water molecule are displayed.

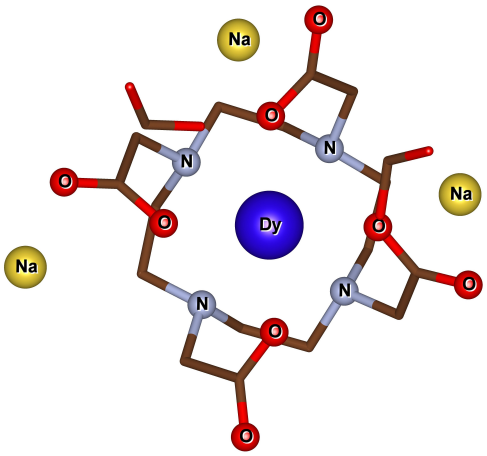

Fig. S4: Model **M3**. Hydrogens atoms and the AWM are hidden for sake of clarity.

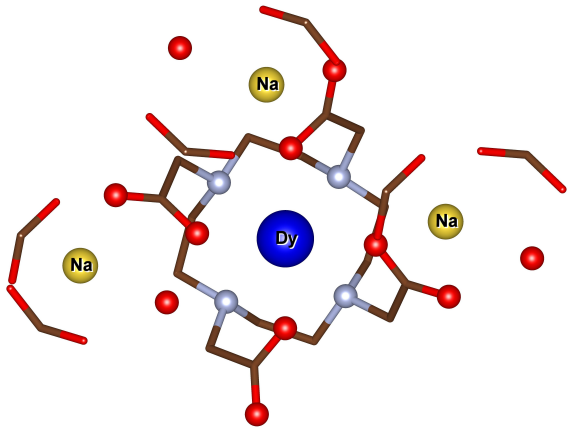

Fig. S5: Model **M4**. Hydrogens atoms and the AWM are hidden for sake of clarity.

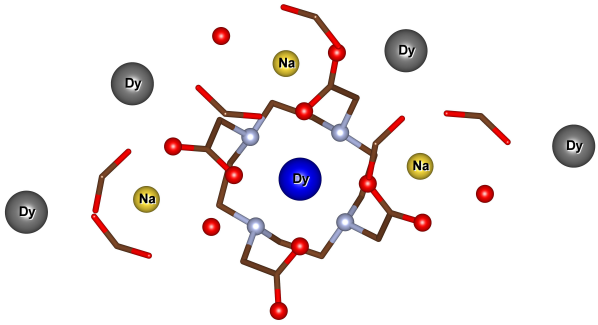

Fig. S6: Model **M5**. The dysprosium atoms in grey are substutued by their atomic point charges. Hydrogens atoms are hidden for sake of clarity.

Table S1: Contractions of the ANO-RCC basis set used for all CASSCF calculations.

Atom	Label	Primitives	Contraction
Dy	VTZP	[25s22p15d11f4g2h]	[8s7p5d3f2g1h]
Na	VDZ	[17s12p5d4f2g]	[4s3p]
N	VTZP	[14s9p4d3f2g]	[4s3p2d1f]
O	VTZP	[14s9p4d3f2g]	[4s3p2d1f]
C	VDZP	[14s9p4d3f2g]	[3s2p1d]
H	VDZ	[8s4p3d1f]	[2s]

Table S2: Results of the calculations on DyDOTA system for the **Models 1,2,3,4,5** and for Model A by Cucinotta *et al.*[1] (two different φ angles) for the optimized position and the one rotated by 90°.

		M1		**M2**		**M3**		**M4**		**M5**		Model A[1] $\varphi = 0°$		Model A[1] $\varphi = 53.6°$	
	Exp	0°	90°	0°	90°	0°	90°	0°	90°	0°	90°	0°	90°	0°	90°
Principal g-values of the ground Kramers' doublet															
g_x	3.4	0.3	1.0	1.0	0.3	0.0	0.2	0.5	0.0	0.1	0.9	0.2	0.5	0.1	1.1
g_y	4.9	0.7	6.1	5.4	0.7	0.0	0.3	1.8	0.1	0.3	4.1	0.9	1.7	0.3	7.1
g_z	17.0	19.2	13.9	14.9	19.1	19.6	19.1	18.0	19.6	19.5	15.6	18.6	18.3	19.5	13.0
γ_0		2.8°	34.1°	8°	81.1°	5.5°	3.5°	88.0°	84.4°	4.6°	11.9°	4.7°	76.7°	0.6°	41.0°
Principal g-values of the first excited Kramers' doublet															
g_x		0.43	1.8	1.7	0.3	0.9	0.3	0.9	0.9	0.7	1.5	0.3	0.6	0.6	1.8
g_y		1.12	4.5	4.4	1.1	1.1	0.8	1.1	0.9	1.0	2.8	1.0	1.3	1.0	5.6
g_z		17.95	11.9	12.9	18.2	18.0	18.1	17.3	18.7	18.4	14.0	18.3	17.3	18.5	11.3
γ_1		80.1°	44.0°	56.1°	4.4°	76.5°	77.5°	8.3°	7.1°	81.0°	67.1°	82.5°	1.1°	85.6°	47.3°
Energy Levels (cm^{-1})															
E_0	0	0	0	0	0	0	0	0	0	0	0	0	0	0	0
E_1	52	47	18	15	39	78	35	16	57	53	15	64	23	48	13
E_2	112	140	123	118	129	132	115	105	120	129	110	112	116	128	111
E_3	198	212	193	185	201	198	173	164	191	193	172	147	183	192	175
E_4	287	298	281	272	289	263	246	246	270	267	250	227	264	269	255
E_5	400	369	352	338	359	307	292	300	328	320	304	284	325	321	309
E_6	454	451	432	412	435	355	344	357	388	378	364	351	395	377	368
E_7	574	590	568	530	561	429	426	437	473	480	471	422	510	472	470

Table S3: Results of the calculations on **M1**, **M2** and Model C by Cucinotta *et al.*[1] without AWM

	Exp	**M1**	**M2**	Model A[1]
		Principal g-values of E_0		
g_x	3.4	0.6	0.7	0.6
g_y	4.9	2.9	3.1	2.9
g_z	17.0	17.3	17.2	17.5
γ_0		3.0°	77.5°	7.6°
		Principal g-values of E_1		
g_x		1.3	1.4	1.3
g_y		1.6	1.7	1.6
g_z		15.7	15.9	16.1
γ_1		76.0°	4.2°	71.2°
		Energy Levels (cm^{-1})		
E_1	0	0	0	0
E_2	52	27	25	26
E_3	112	146	144	143
E_4	198	231	230	223
E_5	287	356	356	343
E_6	400	506	508	483
E_7	454	702	704	670
E_8	574	982	981	941

Model M1: Results

Table S4: Results of the calculations on DyDOTA system for **M1** as a function of α: g-values of ground and first excited Kramers' doublet, corresponding angle between experimental and calculated g_z and energy levels.

	Exp	*Opt*	59°	75°	90°	105°	120°	129°	140°	150°	180°	200°	220°	245°	260°	270°	290°	300°	310°	320°	330°	340°
									Principal g-values of the ground Kramers' doublet													
g_x	3.4	0.3	0.3	0.7	1.0	0.9	0.9	0.9	1.1	0.9	0.3	0.2	0.2	0.6	1.1	1.0	0.8	0.9	1.0	1.1	0.9	0.6
g_y	4.9	0.7	0.9	2.6	6.1	4.5	4.1	5.1	7.1	4.5	0.7	0.5	0.6	2.4	7.3	6.1	3.5	4.2	6.0	8.3	4.8	2.2
g_z	17.0	19.2	19.0	17.3	13.9	15.5	16.0	15.0	13.1	15.7	19.2	19.4	19.3	17.8	13.2	14.3	16.8	16.2	14.5	12.3	15.5	18.0
γ_0		2.8°	1.3°	5.5°	34.1°	67.7°	71.7°	67.8°	34.9°	7.3°	3.5°	3.4°	2.7°	2.2°	25.6°	68.3°	78.5°	77.7°	73.0°	41.5°		1.7°
									Principal g-values of the first excited Kramers' doublet													
g_x		0.43	0.2	0.2	1.8	1.7	1.6	1.7	1.9	1.7	0.4	0.7	0.5	1.0	1.9	1.8	1.6	1.7	1.8	1.9	1.6	0.8
g_y		1.12	1.2	1.2	4.5	3.0	2.6	3.5	5.5	3.1	1.1	1.1	1.1	1.5	5.7	4.4	2.1	2.6	4.3	6.7	3.4	1.5
g_z		17.95	17.6	17.6	11.9	13.8	14.4	13.3	11.1	13.9	18.0	18.1	18.0	16.2	11.2	12.6	15.3	14.7	12.8	10.3	13.8	16.5
γ_1		80.1°	77.5°	73.5°	44.0°	9.2°	5.5°	9.0°	42.9°	72.0°	79.5°	78.7°	78.5°	77.1°	53.5°	9.2°	1.0°	0.9°	4.8°	36.3°		80.0°
									Energy Levels (cm^{-1})													
E_0	0	0	0	0	0	0	0	0	0	0	0	0	0	0	0	0	0	0	0	0	0	0
E_1	52	47	40	25	18	19	20	18	16	18	41	49	44	25	17	18	23	22	19	18	21	28
E_2	112	140	136	128	123	123	122	121	121	122	133	137	135	126	123	124	126	126	125	125	127	131
E_3	198	212	208	198	193	194	194	192	191	192	206	212	209	198	194	195	198	198	197	196	197	201
E_4	287	298	295	286	281	281	281	280	279	280	292	297	295	285	281	282	285	284	283	282	284	288
E_5	400	369	365	357	352	352	351	349	348	349	362	367	366	356	353	354	357	357	356	354	356	359
E_6	454	451	446	437	432	431	430	429	428	428	442	449	449	441	439	440	442	442	440	438	439	442
E_7	574	590	583	574	568	567	566	565	564	565	579	585	585	578	577	578	582	582	580	578	578	581

Table S5: M_J percentage composition of the first two Kramers' doublet for **M1**, $\alpha = 0^\circ, 120^\circ$. The bold numbers are the contributions above 10%.

α	0°	120°
$\|M_J>$	E_0	E_0
$\pm 15/2$	**94.56%**	**24.17%**
$\pm 13/2$	0.03%	2.23%
$\pm 11/2$	0.37%	2.41%
$\pm 9/2$	0.32%	2.51%
$\pm 7/2$	2.37%	6.99%
$\pm 5/2$	0.33%	**11.21%**
$\pm 3/2$	1.27%	**21.80%**
$\pm 1/2$	0.73%	**28.69%**
	E_1	E_1
$\pm 15/2$	2.92%	**70.77%**
$\pm 13/2$	6.58%	2.43%
$\pm 11/2$	3.83%	1.17%
$\pm 9/2$	4.81%	2.07%
$\pm 7/2$	5.16%	1.05%
$\pm 5/2$	**15.61%**	4.45%
$\pm 3/2$	**24.46%**	6.27%
$\pm 1/2$	**36.63%**	**11.79%**

Table S6: M_J composition of the first two Kramers' doublet for **M1** and different α values. The asterisks and the bold numbers are the contributions between 1% and 10% and above 10%, respectively

α	0°	59°	90°	105°	120°
$\|J_M>$	E_0	E_0	E_0	E_0	E_0
$-15/2$	**0.945637794569**	$2.537721E-06$	0.000313313536	**0.58661515957**	0
$-13/2$	$9.7004585E-05$	0.000295706016	∗0.015962307624	∗0.065081643689	0.002478083044
$-11/2$	0.003711116053	$4.4281773E-05$	0.00100378852	**0.128164965442**	0.00010371506
$-9/2$	0.003032620865	0.00026759813	∗0.020024029385	∗0.03060504413	0.008540099956
$-7/2$	∗0.023631617585	0.000131715266	0.001278199858	∗0.044309778869	0.001358255709
$-5/2$	0.001700238005	0.001858448954	∗0.010826768781	∗0.029862839465	∗0.01948399129
$-3/2$	∗0.012328897841	0.000602990408	0.00227782053	∗0.04769606036	0.001543747185
$-1/2$	0.00059979554	0.00970964914	0.0059715553	0.003313736596	∗0.030205776116
$1/2$	0.006733273025	0.001725093316	0.002256339322	∗0.02486049649	0.003855467521
$3/2$	0.000385226794	∗0.017368595152	∗0.021541513925	0.00141136729	∗0.05317234856
$5/2$	0.001585509284	0.003003969258	∗0.013042161205	∗0.02077396885	∗0.020746656122
$7/2$	$7.56697E-05$	∗0.029485855373	**0.130825082169**	0.002163287696	∗0.035553514354
$9/2$	0.000241558241	0.001765765508	0.009096047941	∗0.01200565129	∗0.032372390705
$11/2$	$3.9966845E-05$	0.005407744954	**0.411863760034**	$9.806152E-06$	∗0.076535065828
$13/2$	0.000180669008	0.001019690514	∗0.022165656805	0.003116294869	∗0.053657997236
$15/2$	$1.9722481E-05$	**0.9273112209**	**0.331551398025**	$8.832784E-06$	**0.660391896025**
	E_1	E_1	E_1	E_1	E_1
$-15/2$	$3.1865E-07$	∗0.040789762897	∗0.031937296628	0.00038785482	0.001479623113
$-13/2$	∗0.041645587108	∗0.042041385373	∗0.023887126213	∗0.020995451789	∗0.017375641362
$-11/2$	0.007696600729	∗0.036455187092	∗0.027387688402	0.0002645829	0.000463066673
$-9/2$	∗0.02941911034	∗0.031259804869	0.00556341125	∗0.073580271876	∗0.057891563245
$-7/2$	0.007858168957	∗0.041861995445	0.000159516333	∗0.017262028325	0.008045204714
$-5/2$	**0.145103301608**	∗0.045935065993	0.002260373825	∗0.098323146197	**0.100564125668**
$-3/2$	0.007957554181	**0.21895237861**	0.002284283945	0.0053170021	0.00321069376
$-1/2$	**0.356985253229**	∗0.040599897809	0.00757299176	∗0.082099551626	**0.128106780125**
$1/2$	0.009335749268	**0.308994376181**	0.006191467565	∗0.027670937809	∗0.041975501441
$3/2$	**0.23664901268**	∗0.013454715137	0.003824654665	**0.128499608889**	**0.167298898432**
$5/2$	∗0.010974688394	**0.109129282837**	∗0.075892780772	∗0.09098786698	**0.100719910705**
$7/2$	∗0.043745381098	∗0.008481071537	∗0.043066057513	**0.15823166377**	**0.133622211025**
$9/2$	∗0.018706420017	∗0.021012207506	**0.374042984474**	∗0.036576026728	∗0.013533088221
$11/2$	∗0.030582554138	0.005276902586	0.002501247073	$8.4831025E-05$	0.000856305713
$13/2$	∗0.02412267688	∗0.03574032109	**0.393425341517**	∗0.087706229096	∗0.05574356586
$15/2$	∗0.029218090489	$1.5752961E-05$	$2.436721E-06$	**0.172012585536**	**0.169115047696**

Model M2: Results

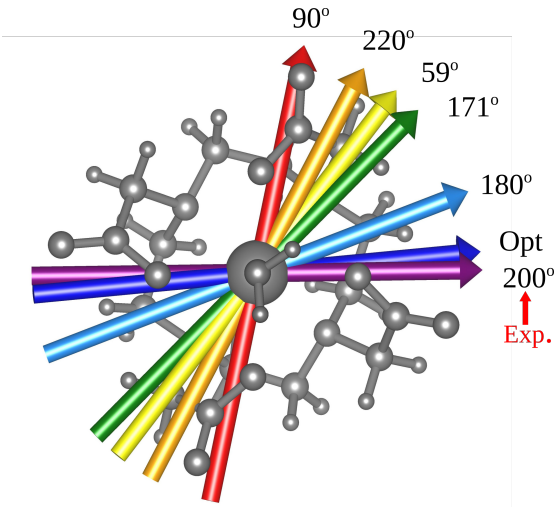

Fig. S7: Orientation of the main magnetic axis for **M2** as a function of α.

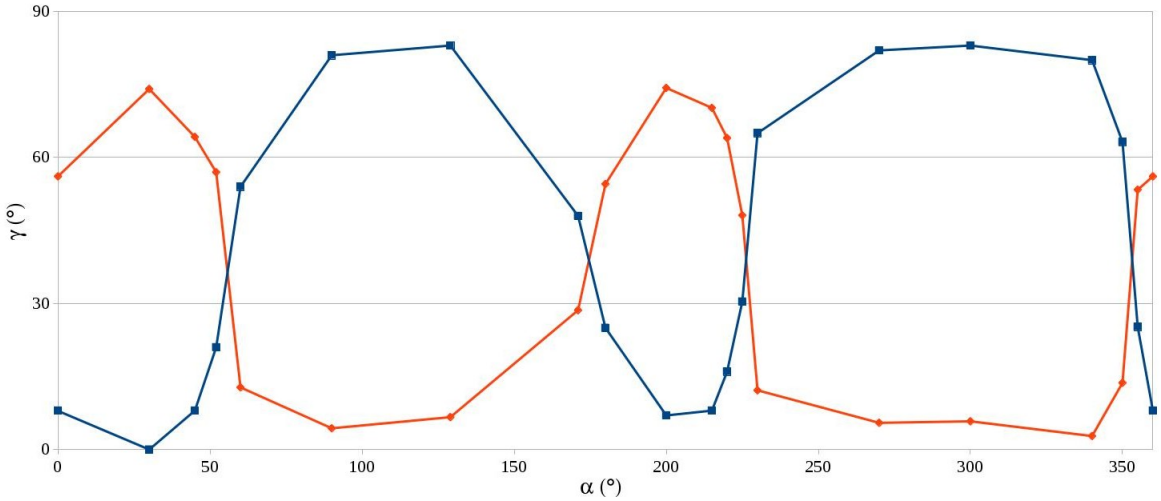

Fig. S8: **M2**. Angle between the calculated and the experimental main magnetic axis as a function of α, for ground and first excited Kramers' doublet

Table S7: Results of the calculations on **Model 2** as a function of α: g-values of ground and first excited Kramers' doublet, corresponding angle between experimental and calculated g_z and energy levels.

	Exp	0°	30°	45°	52°	59°	90°	129°	171°	180°	200°	215°	225°	229°	270°	300°	340°	350°	355°
Principal g-values of the ground Kramers' doublet																			
g_x	3.4	1.0	0.6	0.9	1.0	1.0	0.3	0.2	1.1	1.1	0.8	1.0	1.0	1.0	0.2	0.2	0.7	1.1	1.1
g_y	4.9	5.4	2.3	4.2	6.2	6.4	0.7	0.5	8.0	7.6	4.0	4.9	7.0	5.6	0.5	0.4	2.7	6.9	7.4
g_z	17.0	14.9	17.7	16.0	14.0	13.8	19.1	19.3	12.6	12.9	16.3	15.5	13.3	14.6	19.3	19.4	17.4	13.4	13.9
γ_0		8°	0°	8°	21	54°	81.1°	82.9°	47.8°	24.6°	7.3°		30.4°	65.3°	82.2°	83.3°	79.8°	63.2°	25.2°
Principal g-values of the first excited Kramers' doublet																			
g_x		1.7	1.1	1.5	1.7	1.8	0.3	0.5	1.8	1.8	1.6	1.7	1.7	1.7	0.5	0.8	1.4	1.8	1.8
g_y		4.4	1.3	2.8	4.7	5.5	1.1	1.1	6.7	6.1	2.6	3.4	4.4	4.2	1.1	1.1	1.5	5.4	6.0
g_z		12.9	16.4	14.5	12.1	11.4	18.2	18.4	10.4	11.0	14.6	13.7	12.6	13.0	18.4	18.5	16.2	11.8	11.1
γ_1		56.1°	74.1°	64.2°	57.0°	12.8°	4.4°	6.7°	28.6°	54.6°	74.3°	70.2°	48.1°	12.2°	5.5°	5.8°	2.8°	13.7°	53.4°
Energy Levels (cm^{-1})																			
E_1	0	0	0	0	0	0	0	0	0	0	0	0	0	0	0	0	0	0	0
E_2	52	15	22	18	16	16	39	46	15	15	18	17	15	16	45	52	21	14	14
E_3	112	118	122	121	120	120	129	131	120	120	121	120	118	119	131	134	120	117	117
E_4	198	185	192	191	190	190	201	205	190	190	191	190	188	188	205	211	189	175	185
E_5	287	272	280	279	279	279	289	291	278	278	280	278	276	277	292	296	276	272	272
E_6	400	338	346	347	347	348	359	359	346	347	349	348	346	346	363	367	343	338	337
E_7	454	412	421	424	424	425	435	434	424	426	429	427	426	422	444	447	418	412	411
E_8	574	530	543	548	550	551	561	559	554	556	558	555	552	548	570	575	540	532	530

Model M2m: Results

To verify the influence of the two aldehydes and to have a model directly comparable, except for the different φ angle, with the Model C of the article by Cucinotta *et al.*[1], we removed the above mentioned groups from **M2** to obtain **M2m**. The results are reported in Table S8. For what regards the g-values, no significant differences were found with respect to **M2**, confirming all the observed trends of the previous model. Indeed, plotting the variation of the γ_1 angle in function of the α angle (see Fig. S9) the **M2** and **M2m** trends are superimposable suggesting a limited importance of the two aldehydes on the magnetic structure without undermine their role in the orientation of the two H_{AWM} atoms.

The small deviation between Model C and **M2m** on γ_0 for $\alpha = 0°$ can be explained with the different φ values used in the two models (0° in former and 53.6° in latter), since the difference in φ deviation as only a limited effect on E_0 and E_1 of few degrees and cm^{-1}, respectively (see supra). We can conclude that the good agreement between the experi-

mental easy axis orientation and the computed one in **M2m** (Model C) is due to the not decisive reduction of the $E_0 - E_1$ energy gap below the switch activation energy quantum. Therefore, we can consider such a modelization as a good operative approximation to reproduce the experimental energy ladder and the orientation of the magnetic easy axis. As a drawback, it can be very risky to use it to extrapolate magneto-correlation trends without a validation procedure with an accurate model as **M1**. This is the reason why the computed trend of the easy magnetization axis is only roughly similar to the more reliable ones given by **M1** and **M2m**.

As in **M2**, the removal of the water molecule made the easy axis rotate from the experimental orientation to a $\gamma_0 = 78.2°$, still in agreement with the results reported[1]. A very similar ladder to **M2** has been found as expected (the two aldheyds were too far from Dy(III) to produce a significant effect.

Table S8: Results of the calculations on Model **M2m** as a function of α: g-values of ground Kramers' doublet, corresponding angle between experimental and calculated g_z and energy levels.

	Exp	*Opt*	30°	45°	52°	59°	90°	129°	171°	180°	200°	220°	225°	229°	270°	340°	350°	355°
								Principal g-values of the ground Kramers' doublet										
g_x	3.4	1.1	.8	1.0	1.1	1.0	0.3	0.2	1.1	1.1	0.9	1.1	1.1	1.0	0.2	0.7	1.0	1.1
g_y	4.9	7.8	3.9	6.0	7.3	6.1	0.9	0.6	8.0	8.0	4.9	6.8	7.5	6.0	0.6	2.9	6.2	8.0
g_z	17.0	12.8	16.4	14.4	13.3	14.3	19.0	19.2	12.6	12.5	15.5	13.7	13.0	14.4	19.2	17.3	14.3	12.6
γ_0		22.4°	4.3°	14.2°	36.3°	63.7°	81.2°	82.7°	53.3°	32.6°	8.4°	19.7°	36.5°	66°	82.2°	80.4°	72°	74.2°
								Energy Levels (cm^{-1})										
E_0	0	0	0	0	0	0	0	0	0	0	0	0	0	0	0	0	0	0
E_1	52	18	22	19	17	19	43	49	17	17	20	18	18	19	47	25	19	18
E_2	112	128	130	128	128	128	137	139	127	127	128	127	126	127	139	131	129	128
E_3	198	201	204	202	201	202	214	218	200	200	202	201	200	201	217	206	202	202
E_4	287	293	296	294	294	294	305	308	291	291	293	292	292	294	307	297	294	293
E_5	400	369	371	370	369	370	382	383	365	366	368	369	369	369	385	373	370	369
E_6	454	459	460	458	457	457	469	470	452	454	457	458	458	457	476	463	459	459
E_7	574	610	610	608	606	607	618	620	603	604	608	609	609	608	627	615	611	610

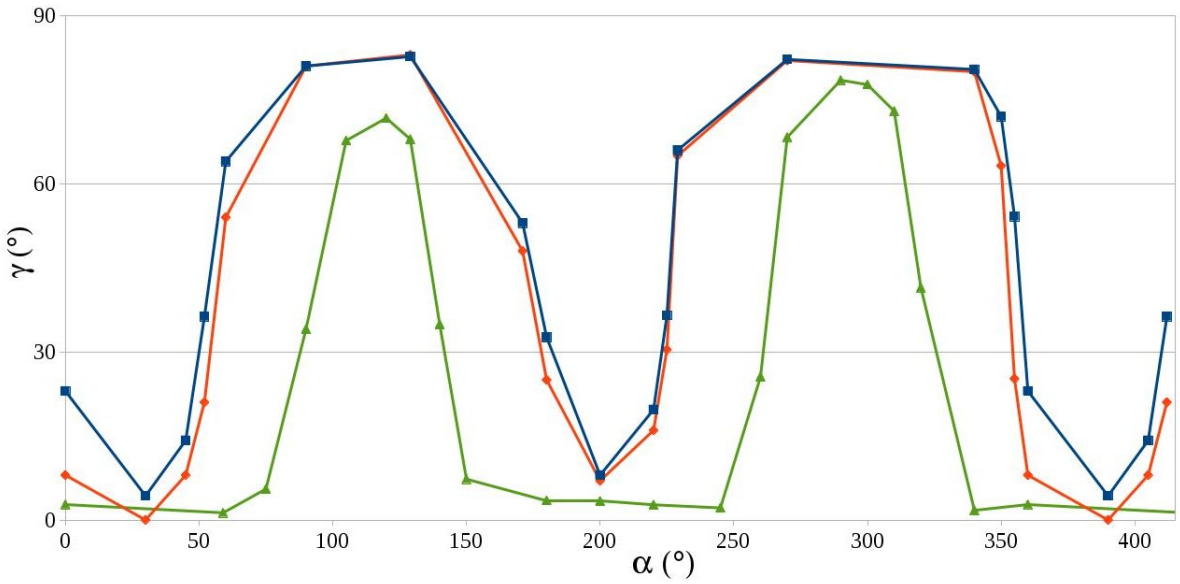

Fig. S9: Angle between the calculated and the experimental main magnetic axis as a function of α for **M1**(green), **M2**(orange) and **M2m**(blue).

Models M3-5: Results and Discussion

Analyzing the computed energy values for the first eight multiplets for **M3-5** models (see Table S2) several important information can be extracted. First of all, comparing the computed trends for the ground and the first excited Kramers' doublets for the three models, it results that the rotation of the AWM has opposite effects on them: strongly destabilizing the former and slightly stabilizing the latter. Such a consideration becomes evident from the E_0 and E_1 values: in **M3** and **M5** the first excited state is stabilized passing from $\alpha = 0°$ to $\alpha = 90°$ while in **M4** becomes, instead, destabilized. Moreover, as already pointed out before, the $(E_{rot1} + E_{cross})$ involved in the AWM rotation for $0° < \alpha < 90°$ was still found similar than in **M1-2** and with slightly differences among the three models: 43 cm^{-1}, 41 cm^{-1}, 38 cm^{-1} for **M3**, **M4**, and **M5**, respectively. The agreement with the experimental E_0 and E_1 values is, however, only quali-tative for **M3** and **M4** while an

excellent agreement was found, instead, for **M5** (see Table S2). The strong dependence on the chosen model is also evident comparing the E_2-E_7 values. In the case of **M3** and **M4** the energy values get lower passing from $\alpha = 0^\circ$ to $\alpha = 90^\circ$ while for **M5** we observed an increase of the energy trends as already found in **M2**. The agreement with the experimental values is good for **M3** and **M5** up to E_4 and it gets worse for higher energies. For **M4** the agreement is overall poorer.

Influence of the Dihedral angle

The influence of the dihedral angle φ was investigated performing single point calculations on model **M2m** (see Tables S9-10). For the two most significant values of the rotation parameter α (0° and 90°) the angle φ was changed into a value of 90° (plane of the water perpendicular to the Dy-O_{AWM} bond) and 180° (plane of the water parallel to the Dy-O_{AWM} bond). It is worth to stress that this last option corresponds to the model published by Cucinotta *et al.*[1] (Model C) on which the magneto-structural correlations where performed. The variation fo the dihedral angle seems not to influence significantly nor the orientation of the main magnetic axes neither the energy ladder. For α equal 0°, the γ_0 angles fluctuates of about 8° around the orientation computed for the otpimized position, with a better agreement with the experimental value found for $\varphi = 180°$. Regarding the energy of the excited states, from E_1 to E_3 the variation is below 10 cm^{-1}, while from E_4 to E_7 the range of variation scales up from 20 cm^{-1} from the fourth excited state to more than 100 cm^{-1} for the seventh one. For α equal 90° geometry, due to the fact thet we have not performed the calculation on the geometry with $\varphi = 180°$, we can only compare with the partial results published by Cucinotta *et al.*[1]: even if we don't have the data for the higher excited states the trend seems the same.

However the dihedral angle influences the flipping process between the two orientations. Cucinotta *et al.*[1] reported that the orientation of the main magnetic axis experiences an abrupt change between the two extreme directions (the experimental and the perpendicular one). The switch is not gradual and happens around 60°, while in our model the process is gradual an at α equal to 60° the magnetization axes experiences an intermediate orientations (vide supra). For this reason calculations were performed varyiing the α angle for a equal $\varphi = 90°$. The results are shown in Table S10. The results are in agreement with

the previous article: when the water molecule is perpendicular to the Dy-O_{AWM} bond the flipping becomes again more abrupt. Indeed at 60° the rotation of the magnetization is only 26° against 54° for the intermediate value of φ, the one we found in the optimized position. The best agreement with the experimental data is again found for 30°. This behaviour could be explained by the increasing of the energy difference between the first two doublets, in analogy with what has already been observed for the different periodicity in **M1** and **M2**. A more accurate mapping of the electronic structure in function of the α angle, i.e. one or two degree instead of 15° as in Cucinotta *et al.*[1], could show again the intermediate position even in a narrower range than **M1**.

Table S9: Results of the calculations on **M2** for dihedral angle $\varphi = 90°, 53.6°, 0°$ for $\alpha = 0°, 90°$.

α			0°			90°	
φ	Exp	90°	53.6°(opt)	0°	90°	53.6°(opt)	0°[1]
Principal g-values of the ground Kramers' doublet							
g_x	3.4	1.1	1.0	0.6	0.4	0.3	0.0
g_y	4.9	7.5	5.4	2.8	1.4	0.7	0.36
g_z	17.0	13.1	14.9	17.3	18.6	19.1	19.19
γ_0		15.1°	8°	3.7°	79.3°	81.1°	86.7°
Energy Levels (cm^{-1})							
E_0	0	0	0	0	0	0	0
E_1	52	18	15	23	36	39	55
E_2	112	127	118	129	137	129	
E_3	198	197	185	203	209	201	
E_4	287	284	272	297	299	289	
E_5	400	361	338	383	375	359	
E_6	454	450	412	486	456	435	
E_7	574	585	530	646	593	561	

Table S10: Results of the calculations on **M2** for dihedral angle $\varphi = 90°$ for different α values.

α	Exp	0°	30°	45°	60°	90°
Principal g-values of the ground Kramers' doublet						
g_x	3.4	1.1	0.6	0.7	1.0	0.4
g_y	4.9	7.5	2.3	3.0	5.7	1.4
g_z	17.0	13.1	17.8	17.1	14.3	18.6
γ_0		15.1°	3.3°	6.5°	26.2°	79.3°
Energy Levels (cm^{-1})						
E_0	0	0	0	0	0	0
E_1	52	18	28	25	20	36
E_2	112	127	134	133	130	137
E_3	198	197	205	205	202	209
E_4	287	284	292	293	291	299
E_5	400	361	368	368	367	375
E_6	454	450	457	456	452	456
E_7	574	585	592	592	588	593

CAMMEL analysis

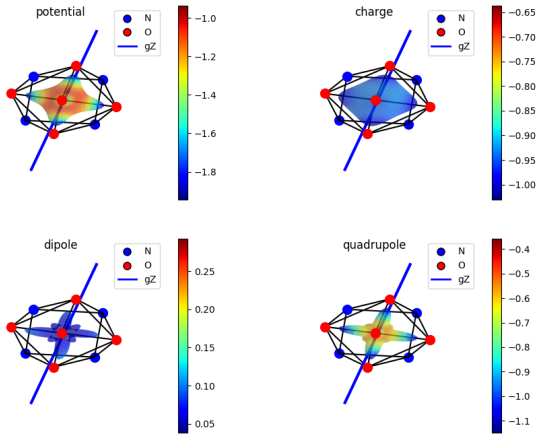

Fig. S10: CAMMEL analysys: Different multipolar contributions of the total electrostatic potential around the Dy(III) ion for **M1** and $\alpha = 0°$, top view. Only the atoms directly bonded to Dy(III) ion are showed. Oxygens and nitrogens are red and blue respectively. The orientation of the easy axis of magnetization for each geometry is also shown.

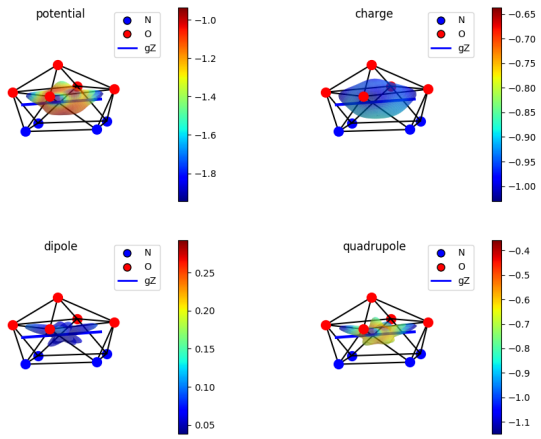

Fig. S11: Model **M1**, $\alpha = 0°$, side view.

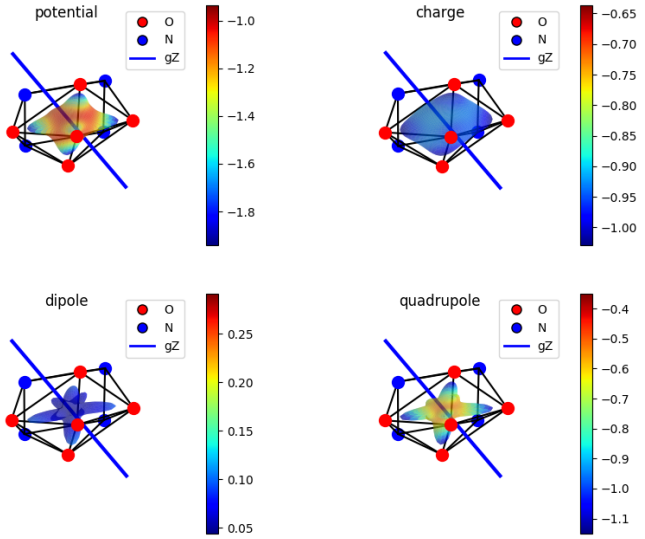

Fig. S12: Model **M1**, $\alpha = 90°$, top view.

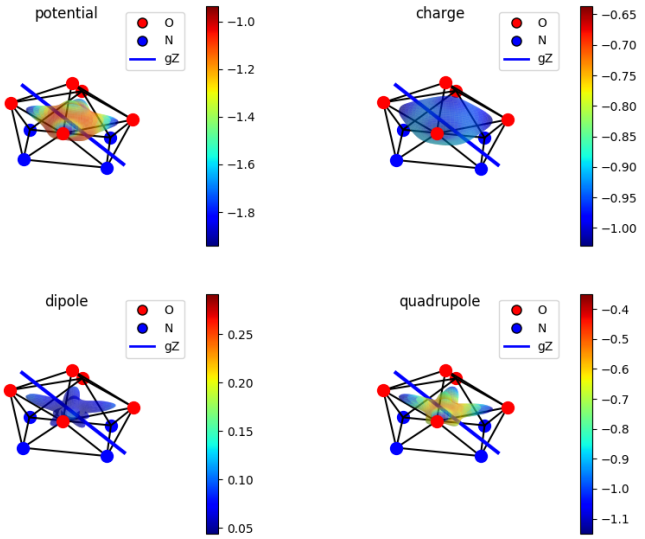

Fig. S13: Model **M1**, $\alpha = 90°$, side view.

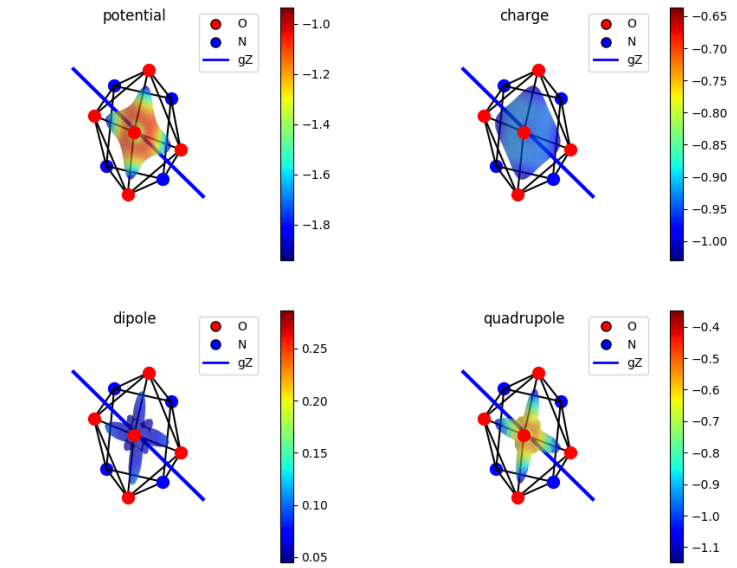

Fig. S14: Model **M1**, $\alpha = 120°$, top view.

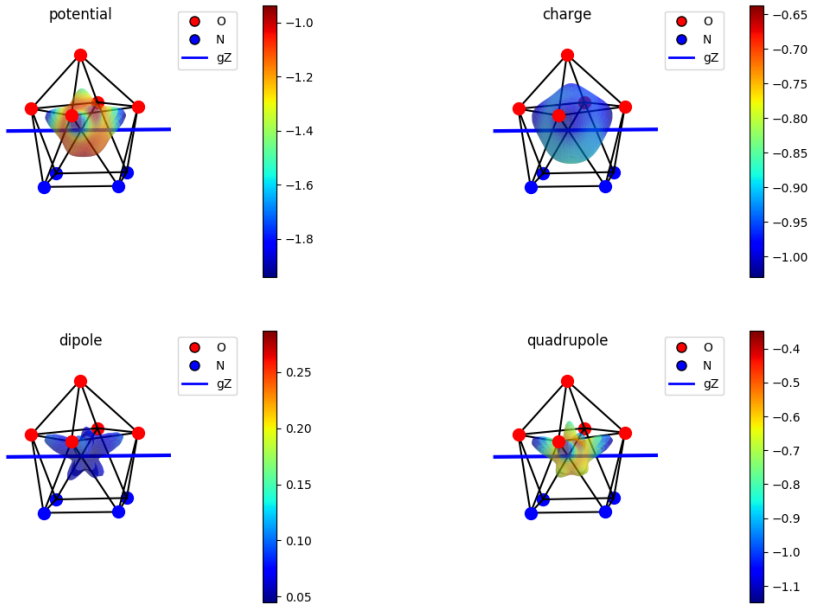

Fig. S15: Model **M1**, $\alpha = 120°$, side view.

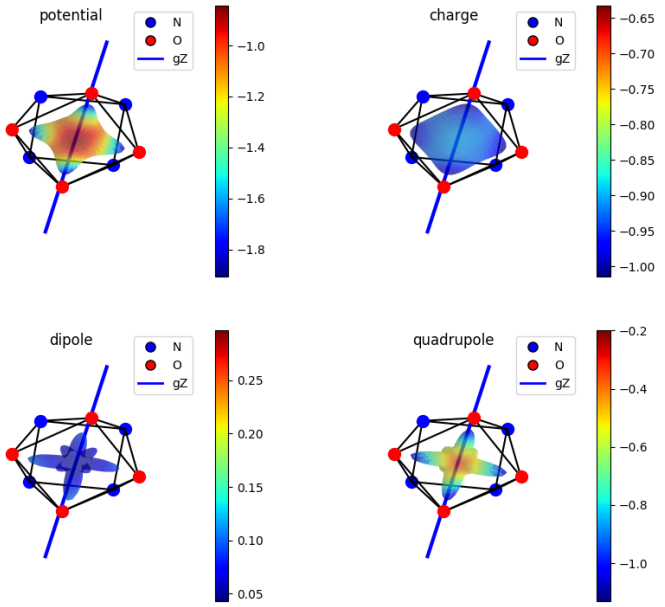

Fig. S16: Model **M1** without the AWM, top view.

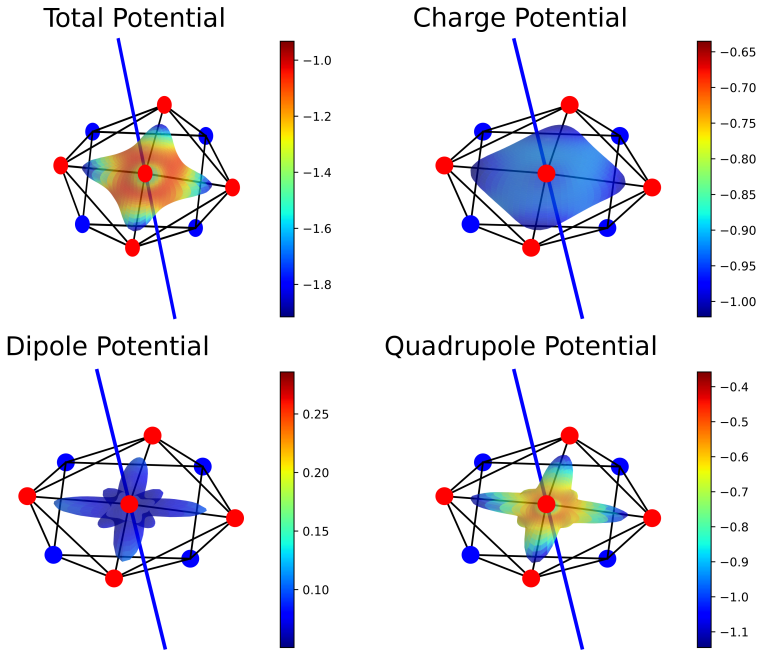

Fig. S17: **M2m** and $\alpha = 0°$.

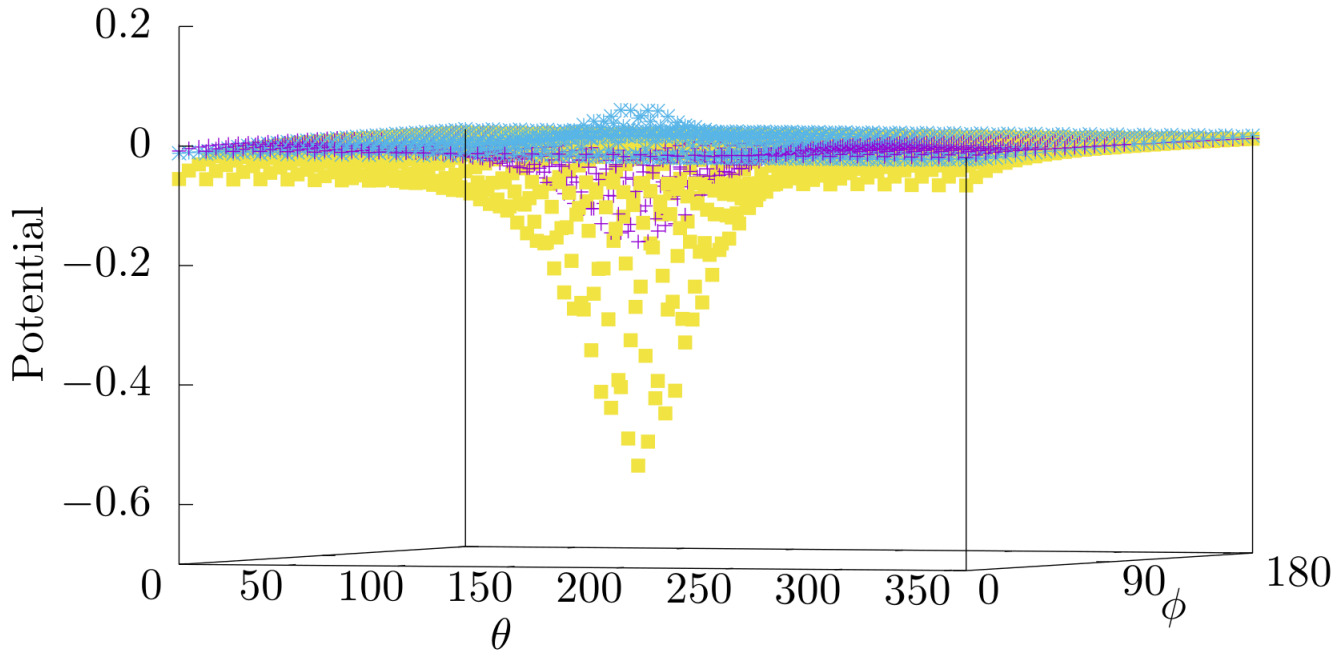

Fig. S18: CAMMEL analysis of the total electrostatic potential of the water molecule directly bonded to the Dy(III) ion for **M1** and $\alpha = 0°$. The potential have been decomposed in the single charge (purple), dipolar (blue) and quadrupole contribution (yellow)

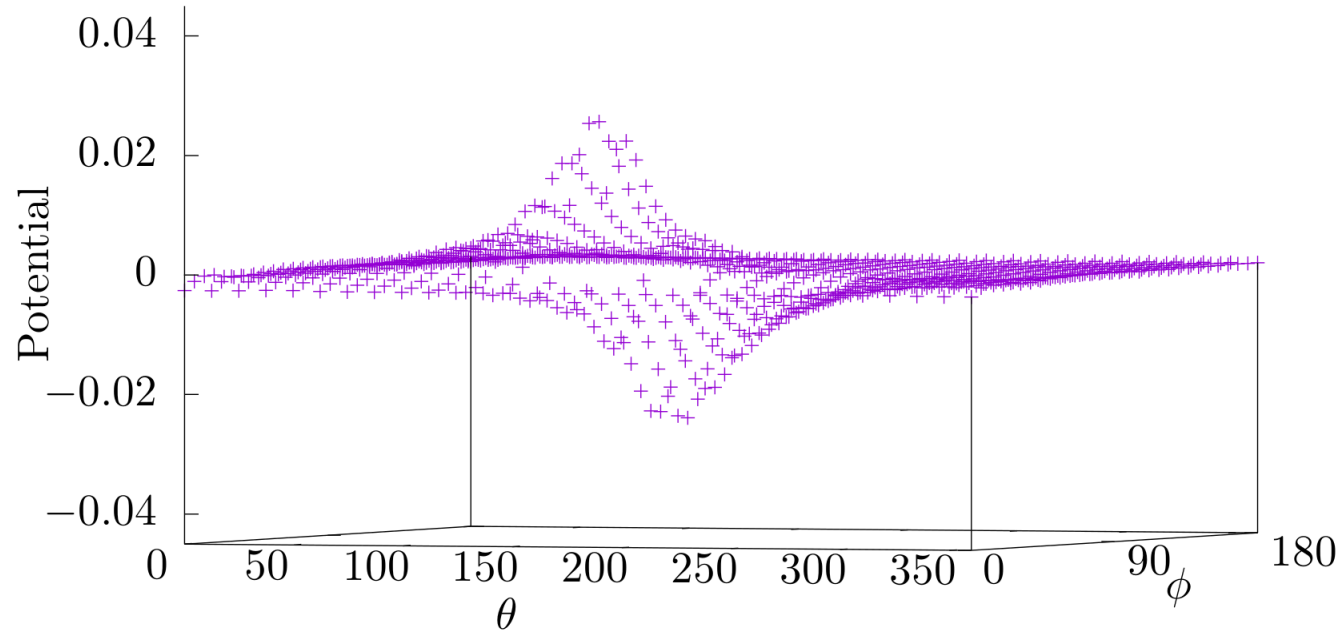

Fig. S19: Differences between the quadrupolar electrostatic field of the AWM, at $\alpha = 0°$, 90°, obtained from CAMMEL analysis, in **M1**.

Calculations Substituing the AWM with LOPROP Moments

Table S11: Results of the calculations on **M1** substituing the AWM with its LOPROP electrostatic multipolar expansion: point charges, dipoles and quadrupoles

		M1						**M2m**					
α		0°(Opt)		90°		120°		0°(Opt)		59°		90°	
	Exp	*Orb*	*Charge*	*Orb*	*Charge*	*Orb*	*Charge*	*Orb*	*Charge*	*Orb*	*Charge*	*Orb*	*Charge*
		Principal g-values of the ground Kramers' doublet											
g_x	3.4	0.3	0.0	1.0	0.1	0.9	0.5	1.1	0.1	1.0	0.3	0.3	0.0
g_y	4.9	0.7	0.1	6.1	0.2	4.1	1.8	7.8	0.6	6.1	0.9	0.9	0.15
g_z	17.0	19.2	19.8	13.9	18.7	16.0	14.6	12.8	19.2	14.3	18.1	19.0	19.5
		Direction Cosines g_z of the ground Kramers' doublet											
a	0.6700	0.684155	0.733288	0.689162	0.7325531	0.419056	0.670775	0.687617	0.703587	0.504959	0.718865	0.338244	0.351829
b'	−0.2920	−0.327447	−0.335766	0.293259	−0.252991	0.816357	0.485637	0.093666	−0.336994	0.726934	−0.226048	0.899246	0.907963
$c*$	0.6826	0.651698	0.591228	0.662612	0.6319511	0.397433	0.560551	0.720007	0.625620	0.465385	0.657370	0.277393	0.227639
γ_0		2.8°	6.8°	34.1°	5.1°	71.7°	46.3°	22.4°	4.5°	63.7°	4.9°	81.2°	82.8°
		Energy Levels (cm^{-1})											
E_0	0	0	0	0	0	0	0	0	0	0	0	0	0
E_1	52	47	58	18	16	20	6	18	18	19	11	43	27
E_2	112	140	131	123	105	122	97	128	107	128	104	137	109
E_3	198	212	181	193	151	194	144	201	153	202	152	214	160
E_4	287	298	261	281	236	281	229	293	238	294	239	305	246
E_5	400	369	335	352	307	351	298	369	311	370	314	382	321
E_6	454	451	422	432	386	430	378	459	395	457	399	469	405
E_7	574	590	529	568	480	566	470	610	491	607	499	618	504

Table S12: Results of the calculations on **M1** for α = 120° substituing the AWM with different multipolar expansions: point charges (PC), dipole (D), point charges and dipole (PC+D), quadrupole (Q), total (PC+D+Q).

α		0°	120°					
	Exp	Orbitals	PC	D	PC+D	Q	PC+D+Q	Orbitals
	Principal g-values of the ground Kramers' doublet							
g_x	3.4	0.3	0.7	0.5	0.5	0.7	0.5	0.9
g_y	4.9	0.7	3.5	1.9	2.1	7.6	1.8	4.1
g_z	17.0	19.2	16.5	18.2	17.8	12.6	14.6	16.0
	Direction Cosines g_z of the ground Kramers' doublet							
a	0.6700	0.684155	0.684684	0.655762	0.679510	0.643919	0.670775	0.419056
b'	−0.2920	−0.327447	−0.182068	−0.278592	−0.245083	0.329497	0.485637	0.816357
$c*$	0.6826	0.651698	0.705733	0.701685	0.691521	0.690507	0.560551	0.397433
γ_0		2.8°	6.5°	1.45°	2.72°	36.2°	46.4°	71.7°
	Energy Levels (cm^{-1})							
E_0	0	0	0	0	0	0	0	0
E_1	52	47	16	31	18	8	6	20
E_2	112	140	124	144	122	110	97	122
E_3	198	212	191	225	185	167	144	194
E_4	287	298	293	344	281	264	229	281
E_5	400	369	403	482	382	372	298	351
E_6	454	451	541	662	506	512	378	430
E_7	574	590	731	919	675	689	470	566

References

1 G. Cucinotta, M. Perfetti, J. Luzon, M. Etienne, P. E. Car, A. Caneschi, G. Calvez, K. Bernot and R. Sessoli, *Angew. Chem., Int. Ed.*, 2012, **51**, 1606–1610.

2 O. A. Blackburn, N. F. Chilton, K. Keller, C. E. Tait, W. K. Myers, E. J. L. McInnes, A. M. Kenwright, P. D. Beer, C. R. Timmel and S. Faulkner, *Angew. Chem, Int. Ed.*, 2015, **54**, 10783–10786.

3 N. F. Chilton, D. Collison, E. J. L. McInnes, R. E. P. Winpenny and A. Soncini, *Nat. Commun.*, 2013, **4**, 2551